AICD and Arc overexpression in drosophila increase APP cleavage and promotes aggregates in the brain

KAIDE ZOU

Troy High School, Harvard University Fullerton, California

Published November, 2025

Abnormal amyloid precursor protein (APP) processing, specifically cleavage through the amyloidogenic pathway, creates amyloid-beta proteins that, when oligomerized, cause brain damage and are a hallmark of Alzheimer's disease. Here, we examined how AICD and Arc expression affect APP localization and processing in Drosophila. Immunohistochemistry revealed that AICD overexpression induced Arc expression and led to APP clustering and accumulation, which were not present in controls. Western blot analysis showed that Arc-GFP expression generated additional APP-related species, possibly by- products of APP proteolysis. This included AICD, which drives the feed-forward loop in APP cleav- age and Alzheimer's disease. Furthermore, long-term memory (LTM) training increased APP cleavage in MBON-5β neurons, which in turn caused increased AICD and sAPP levels. These findings suggest that Arc and AICD are the main components in APP proteolysis, and memory-related activity further drives the feed-forward loop in vivo.

1. INTRODUCTION

The amyloid cascade hypothesis has been the hallmark of Alzheimer's disease (AD) research for many decades. Amyloid-beta plaques accumulate in the brain, leading to a series of events that cause neuronal damage (Golde et al. 252). Primarily, these plaques form neurofibrillary tangles composed of the tau protein. While tau proteins are naturally occurring structural stabilizers in the brain, they can cause severe problems when hyperphosphorylated, such as disrupting neuronal communication and causing loss of brain function (National Institute on Aging). This is consistent with the observed physical dysfunctions in patients affected by Alzheimer's disease, in whom decreases in cognitive function and memory recall result from the inability of neurons to communicate.

The creation of amyloid-beta peptide (Aβ) occurs through a series of proteolytic processes on another protein, the amyloid precursor protein (APP) (Chen et al. 1205). APP is a natural transmembrane protein that is broadly expressed during brain development. It supports neuronal proliferation and differentiation and is also involved in synapse formation (Zheng and Koo 27). When cleaved, an extracellular domain of the APP protein, sAPPα, is generated, taking on a neuroprotective role and regulating neuronal health (Nhan et al. 1). Therefore, these proteolytic processes are naturally occurring without viral or bacterial intervention and are not subject to DNA mutations or irregularities. However, this cleavage is carried out by α-secretase in the middle of the fragment containing Aβ, maintaining the regular cellular functions found in humans without AD (Asai et al. 231). When APP is cleaved through the amyloidogenic pathway, the protein is processed by two other secretases: β-secretase (BACE1) at the N-terminus of the Aβ region and γ-secretase for the remaining segment (Hur 433). This is important because β-secretase cleavage allows Aβ to remain intact. Additional fragments are created through this proteolytic process, including sAPPβ, which is an inferior version of its alpha counterpart; a transmembrane protein with toxic properties to neuronal cells called C99; and, crucially, the intracellular component AICD (Orobets and Karamyshev 14794).

Once cleaved, the AICD fragment moves away from the membrane towards the center of the cell. There, it goes into the nucleus and becomes a transcription factor (Müller et al. 393). Inside the nucleus, important genes are upregulated, including the GSK-8B and BASE1. GSK-8B is a gene that codes for a crucial kinase important in tau phosphorylation regulation (Chang et al. 4327). Previously mentioned, hyperphosphorylation of the tau protein produces neurofibrillary tangles that block synaptic signaling. BASE1 is the gene that encodes the β-secretase present in the proteolytic processes of the APP. A feed-forward loop is then created, where an upregulation of β-secretase causes an increase in cleavage, producing the harmful Aβ (Doig 25). AICD production is also increased by the upregulation of the secretase.

The Activity-regulated cytoskeleton associated protein (Arc protein) is a protein vital in synaptic plasticity, neural learning, and memory formation. It is expressed in neuronal cells in response to activity across the synapses and is critical for Long-term potentiation (LTP) and memory consolidation. Stud-

ies have shown elevated Arc levels within brains of Alzheimer's patients. In drosophila tauopathy models, tau overexpression increases Arc1 expression, a fly homolog (Schulz et al. 101). Moreover, Arc plays a role in a theory developed in the early 20th century, the Virus-like particle (VLP) theory. The protein contains a retrovirus-derived Gag domain, which allows it to create capsids contained with its own mRNA. This Arc mRNA capsid can be transferred between neurons, inducing endocytosis and mimicking viral infection in neuronal cells (Ashley et al. 262). This ties in with AD because once tau protein becomes hyperphosphorylated, it disrupts a key process that keeps Arc mRNA levels in check called the nonsense-mediated mRNA decay. The end result is an accumulation of Arc1 mRNA, causing overproductions of Arc and VLP formation. In brains without AD, Arc VLP regulates synaptic plasticity, but an overaccumulation of Arc VLP leads to synaptic weakening.

The direct relationship and feedback regulation have not been characterized to a full extent in drosophila melanogaster. Here, we use Drosophila as a model to connect Arc-driven neuronal activity with AICD-mediated transcriptional feedback in APP processing, which enables investigation of the ARC-AICD feedforward loop. By linking these pathways, this study extends prior findings into a physiological context and introduces a new model for the mechanisms in Alzheimer's disease.

2. METHODS

Immunohistochemistry: dissections were performed on third instar Drosophila melanogaster larvae in 1× phosphate-buffered saline (PBS) without detergent. Brains were immediately transferred to 4% paraformaldehyde in phosphate buffer and fixed for a minimum of 1 hour at room temperature or overnight at 4 °C. After fixation, brains were washed 3× with PBS containing 0.3% Triton X-100 (PBT) to permeabilize cell membranes. Samples were then blocked in 10% normal serum (goat or horse, as indicated by experiment) in PBT (PBTN) for 1 hour at room temperature to reduce nonspecific antibody binding. Brains were incubated in primary antibody diluted in PBTN for at least 4 hours or overnight at 4 °C. After primary incubation, samples were washed three times for 25 minutes each in PBT. To minimize background during secondary staining, brains were re-blocked in PBTN for 30 minutes. Fluorophore-conjugated secondary antibodies were applied in PBTN for a minimum of 4 hours or overnight at 4 °C. Final washes (3× in PBT, 25 minutes each) were conducted to remove unbound antibody. Brains were then mounted in Vectashield and imaged by confocal microscopy. All confocal images were acquired using a Zeiss LSM 780 with a 63× Plan-Apochromat 1.4 NA DIC oil immersion objective. Images were taken using identical acquisition settings across experimental groups. Quantification of fluorescence signal was performed using ImageJ software

Description of the experiment parameters of IHC

Western blot: Frozen Drosophila melanogaster heads were homogenized in 2× laemmli sample buffer at 15 µL per head and boiled at 95 °C for 10 minutes to denature proteins. After brief centrifugation, equal amounts of protein (~20 µg per lane) were loaded onto 4–20% SDS-PAGE gels and electrophoresed using Tris-Glycine-SDS running buffer. Gels were initially run at 50 V for 5 minutes and then at 100–150 V for approximately 1 hour. Following electrophoresis, proteins were transferred to nitrocellulose membranes in Tris-Glycine transfer buffer containing 20% methanol. For proteins larger than 80 kDa, SDS was included in the transfer buffer at 0.1% final concentration. Transfers were performed either at 100 V for 1–2 hours or overnight at 10 mA constant current in a cold room. Membranes were briefly stained with Ponceau S (0.2% in 5% glacial acetic acid) to verify transfer quality, then rinsed and blocked in 3% BSA in TBST (20 mM Tris-HCl pH 7.5, 150 mM NaCl, 0.1% Tween-20) for 1 hour at room temperature. Primary antibody incubation was performed overnight at 4 °C in blocking buffer. Blots were then washed 3–5 times for 5 minutes each in TBST and incubated with HRP-conjugated secondary antibodies for 1 hour at room temperature. After further washes, chemiluminescent detection was carried out using SuperSignal West Femto substrate. Signal was captured using a CCD camera-based ChemiDoc system (Bio-Rad). Band intensities were quantified using Image Lab software and normalized to total protein or a loading control.

All samples were carefully normalized for protein expression levels in order to ensure that observed differences in APP cleavage were not the results of confounding variables. Equal total protein (~20 µg per lane) was verified prior to electrophoresis. Band intensities were normalized to β-actin as a loading control. Furthermore, Arc-GFP and ACID transgenes were under identical Gal4 promoters. Membranes were imaged under identical exposure settings through the ChemiDoc system. These controls confirm that differences in APP processing came from Arc-GFP or AICD activity instead of expression variability.

3. RESULTS OF IHC

In order to examine the effects of AICD overexpression on APP localization and cleavage, immunohistochemistry (IHC) was performed using anti-APP and anti-Arc primary antibod- ies in control and AICD overexpressing samples of drosophila melanogaster brains (see Table 1 for specifics). The primary antibodies were conjugated with secondary antibodies, where APP is visualized with a Cy3 secondary (red) and Arc with a Cy5 secondary (blue). Samples were imaged via confocal microscopy to assess protein localization in control and AICD samples.

Fig. 1A Posterior Brain Region - Sample Back 1

In control brains, APP signal (red) appeared evenly distributed across the tissue with no significant accumulation or localization. Arc signal was absent, as expected in the absence of AICD. Quantification revealed that mean APP signal intensity decreased significantly in AICD-overexpressing brains compared to control (from ~40 to ~18 arbitrary units), despite the structured reorganization observed (Fig. 1E). In AICD-overexpressing brains, strong Arc signal was observed throughout the central region of the tissue, indicating successful induction of Arc protein expression. Within these Arc-enriched regions, APP staining showed further concentration and organization into structured patterns. Notably, Region A displayed ring-like halos surrounding Arc-expressing cells. In Region B, red fluorescence appeared along peripheral areas with reduced Arc expression, possibly suggesting APP aggregation or accumulation of cleaved fragments.

Fig 1B. Posterior Brain Region - Sample Back 2

The control samples were consistent with Back 1 with diffuse APP staining but minimal Arc signal, and AICD samples displayed Arc accumulation in a bilobed structure. In Region C, Arc was robustly expressed throughout the dorsal lobe and also accompanied by an enhanced pericellular APP signaling. Moreover, in Region D, APP and Arc co-localized around a ventral subdomain, which suggests a distinct spatial regulation in subpopulations of Arc-expressing neurons. Quantitative analysis

Experiment	Genotype(s)	Blocking Serum	Primary Antibodies	Secondary Antibodies
IHC Round 1	OK107 vs. OK107 > UAS-Arc	Horse	anti-APP (-20) (1:500), anti-Arc (1:500)	Cy3 anti-chicken (1:500), Cy5 anti-rabbit (1:400)
IHC Round 2	5b,OK107 vs. 5b,OK107 × UAS.Arc1	Goat	anti-APP (-20) (1:500), anti-Arc (1:500)	FITC anti-chicken (1:500), Cy3 anti-rabbit (1:400)

Table 1: Description of the experiment parameters of IHC

Experiment	Genotype(s)	Primary Antibody	Dilution (Primary)	Secondary Antibody	Dilution (Secondary)
WB Exp 1	OK107 vs. Arc-GFP	αAPP (-80)	1:1,000	α-chicken HRP	1:10,000
WB Exp 2	5b no LTM vs. 5b LTM	αAPP (-20)	1:2,000	α-chicken HRP	1:2,000

Table 2: Description of the experiment parameters of Western blot

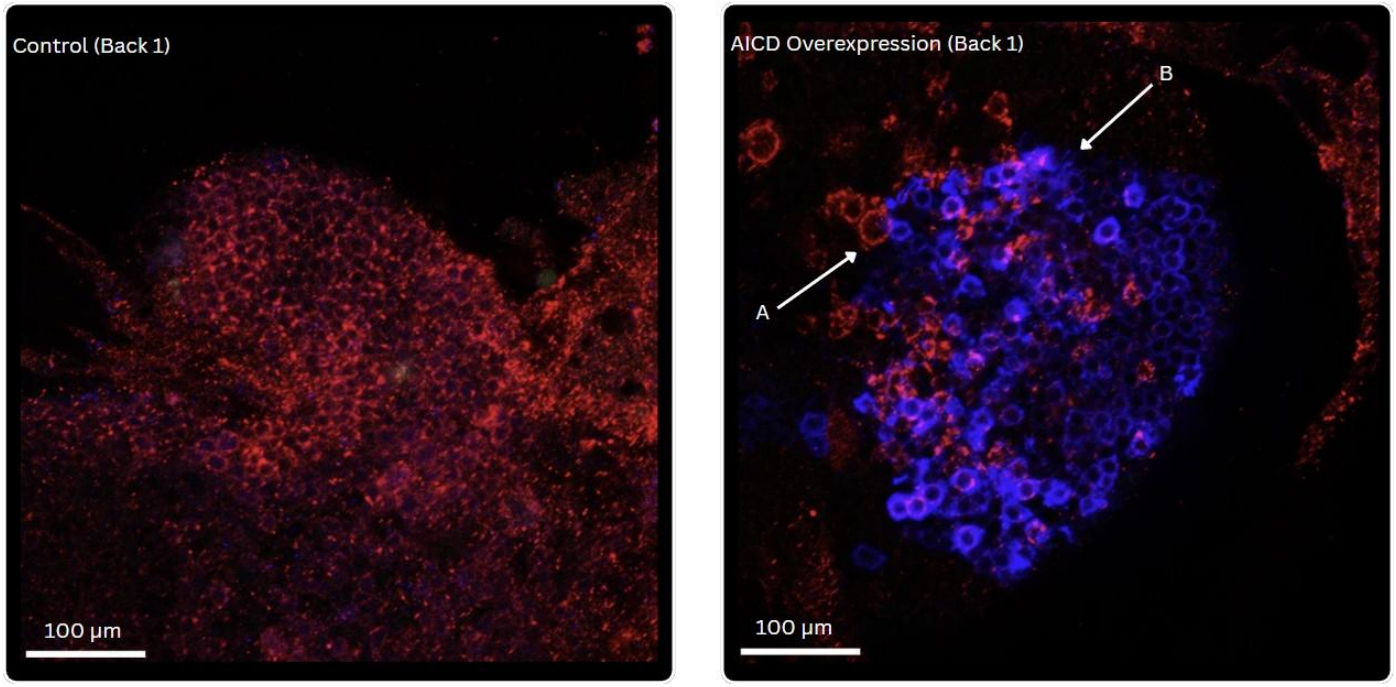

Fig. 1A. Posterior brain region (mushroom body lobe). APP (red) and Arc (blue) staining in control vs AICD-overexpressing brains. AICD induces Arc expression and promotes APP clustering around Arc-positive neurons.

showed a substantial drop in APP intensity in AICD-expressing brains, from ~61 to ~33 units. This suggests a loss of global APP signal intensity in the posterior brain despite focal APP enrichment around Arc-expressing zones (Fig.1E).

In control anterior brain sections, APP staining remained diffuse with little detectable Arc expression. In contrast, AICD-overexpressing brains showed distinct Arc-positive neuronal clusters. In Region E, Arc signal was confined to a discrete circular structure, surrounding APP signal appeared enriched, suggesting localized APP accumulation near Arc-expressing domains . Quantification confirmed a striking increase in APP signal intensity, from ~25 units in control brains to ~54 in AICD-overexpressing samples. This supports the visual observation of Arc-guided APP enrichment in the anterior brain (Fig.1E).

Control samples exhibited low APP intensity with no distinct structural organization. In AICD-overexpressing brains, a well-defined Arc-positive region emerged in the anterior domain. In Region F, APP fluorescence appeared enhanced and layered along the Arc-expressing structure. A notable detail is that the APP signal was sharply defined at the boundaries of Arc accumulation, suggesting that Arc expression may contribute to subcellular partitioning or trafficking of APP. Quantitative data revealed a comparable increase in APP intensity, rising from ~22 in control to ~55 in the experimental group. This aligns with the anterior-specific APP elevation observed in confocal imaging and suggests region-dependent effects of AICD overexpression on APP distribution (Fig.1E).

4. CONCLUSION

Consistently observed across all imaged brain regions, AICD overexpression induced Arc protein expression and was associated with a redistribution of APP signal. However, AICD-expressing brains exhibited Arc-dependent APP clustering, pericellular ring formation and regional accumulation, which contrast with the diffuse APP staining in controls.

5. RESULTS OF WESTERN BLOT 1

To assess whether Arc-GFP expression affects APP protein levels and cleavage, we performed Western blotting on lysates from control (OK107) and Arc-GFP–expressing Drosophila brains. Samples were treated with an anti-APP (-80) antibody (1:1,000) and visualized using an anti-chicken secondary antibody (1:10,000).

In control samples, a single faint band was detected at approximately 130 kDa, corresponding to a full-length APP. No additional bands were visible, which indicates expected minimal APP processing (see Fig. 2A).

In contrast, brains expressing Arc-GFP exhibited multiple distinct bands. The 130 kDa band was clearly more intense, which indicates an increase in full-length APP levels. However, a second molecular band at a higher weight, ~180 kDa, was also observed in the Arc-GFP condition, potentially representing a protein complex between APP and Arc-GFP or APP oligomerization.

Two additional lower-molecular-weight bands were identified: A ~50 kDa band, which may represent a cleaved APP C-terminal fragment (e.g., AICD) possibly stabilized by interaction with Arc-GFP. A ~25 kDa band, consistent with the expected size of Arc-GFP alone. These bands were absent in control lanes, supporting their specificity to Arc-GFP expression. Quantification of band intensities revealed that Arc-GFP expression reduced full-length APP levels (0.4 a.u. vs. 1.0 a.u.) and increased AICD signal (1.5 a.u. vs. 0.2 a.u.) compared to control. These results indicate enhanced cleavage of APP under Arc-GFP conditions. No significant signal was observed for intermediate cleavage fragments in the control group. A ~25 kDa band, consistent with Arc-GFP alone, was detected exclusively in the Arc-expressing group (see Fig. 2B).

6. CONCLUSION

Together, these findings indicate that Arc-GFP expression increases APP levels and is associated with the appearance of additional APP-related species, including a potential high molecular weight complex and cleaved products. These results suggest that Arc-GFP does indeed alter APP processing in the Drosophila brain.

7. RESULTS OF WESTERN BLOT 2

To investigate whether Arc1 expression affects APP processing in MBON-5β neurons, we performed Western blot analysis on fly brain samples expressing UAS.Arc1 under the control of the 5b and OK107 drivers. Protein lysates were probed with an anti-APP antibody to evaluate differences in full-length APP and its cleavage products. Distinct bands were observed at ~130–140 kDa, which corresponds to full-length APP, as well as at ~100 kDa and ~30–35 kDa, representing soluble APPα/β (sAPP) and the APP intracellular domain (AICD) respectively. Arc1-overexpressing flies exhibited a notable reduction in the full-length APP band and an increase in AICD and higher-molecular-weight APP complexes (~180 kDa) compared to the control, which suggests an increase in cleavage (see Fig. 3A).

Quantification of band intensities revealed that Arc1 overexpression reduced full-length APP levels (0.7 a.u. vs. 1.0 a.u.) and increased AICD/RFP signal (1.25 a.u. vs. 0.45 a.u.) compared to control. sAPP levels were modestly elevated (1.0 a.u. vs. 0.5 a.u.), and the ~180 kDa APP cluster band showed a pronounced increase under Arc1 expression (see Fig. 3B).

These results indicate that Arc1 promotes APP cleavage and influences APP trafficking and formation within MBON-5β neurons, which potentially alters downstream signaling pathways implicated in neurodegenerative processes.

8. DISCUSSION

The study demonstrates that Arc and AICD overexpression does indeed have a significant influence on APP processing and distribution seen in samples of transgenic drosophila brains.

IHC analysis revealed that AICD induces Arc protein expression across multiple different brain regions, and along with it a redistribution of APP signaling. Brains expressing AICD ex- hibited Arc-dependent APP clustering, which are unlike the diffuse APP staining observed in controls. Additionally, for- mation of organized structures and accumulation suggest that AICD may modulate synaptic membrane-associated trafficking of APP, and is actively involved in increasing APP cleavage rates and continuing the feed-forward loop.

Western blot analysis showed that Arc-GFP expression in drosophila brains leads to the emergence of additional APP-related bands. These bands include a ~180 kDa band, which potentially correlate to APP-Arc complexes or multiple APP oligomerized together. This consistent appearance of the ~180 kDa band suggests that it represents a different biochemical state

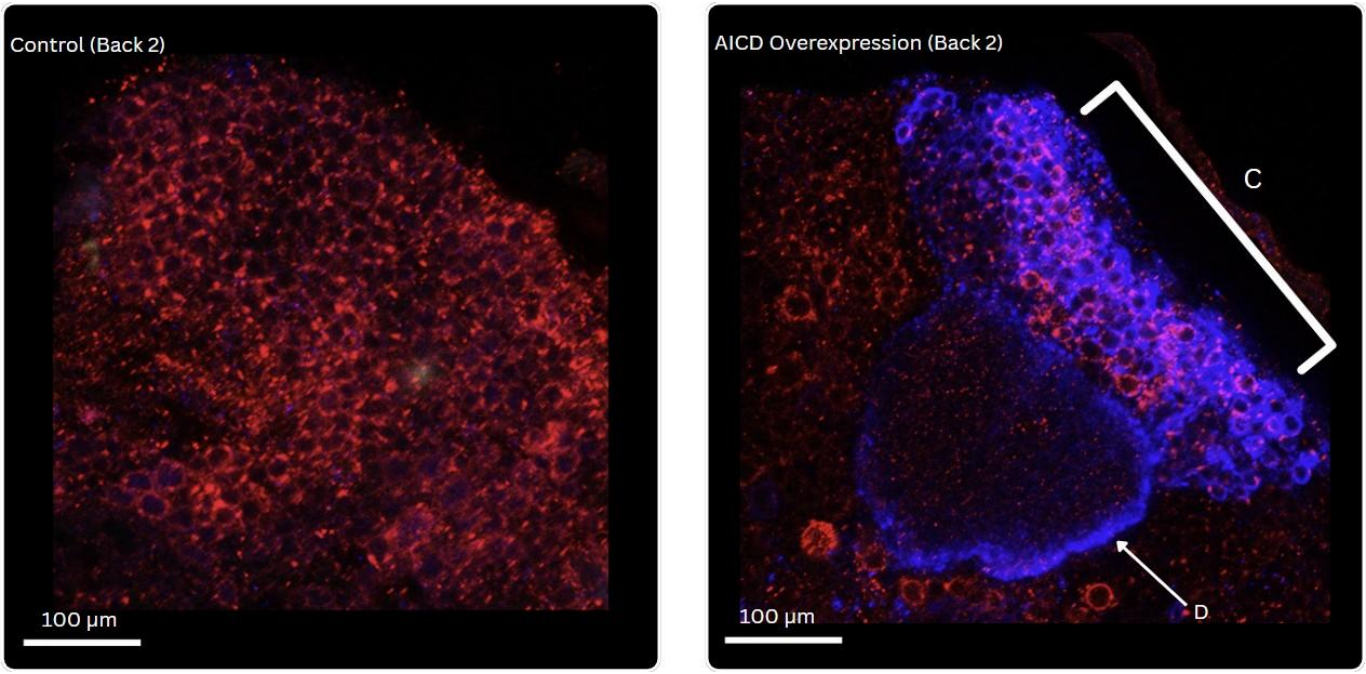

Fig. 1B: Posterior brain region (bilobed lobe). Control vs AICD-overexpressing brains show Arc accumulation and localized APP enrichment near Arc-expressing zones despite reduced overall intensity.

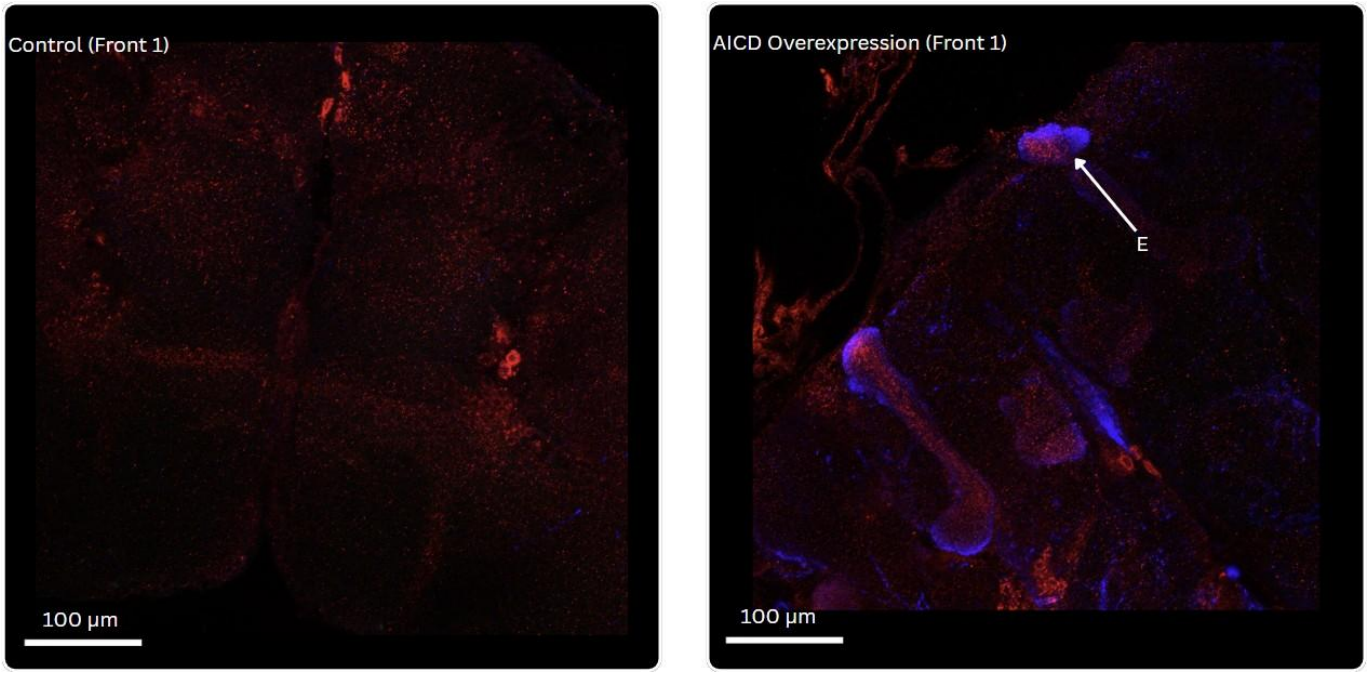

Fig. 1C: Anterior brain region. AICD overexpression produces Arc-positive clusters with elevated APP surrounding Arc do- mains, indicating Arc-guided APP accumulation.

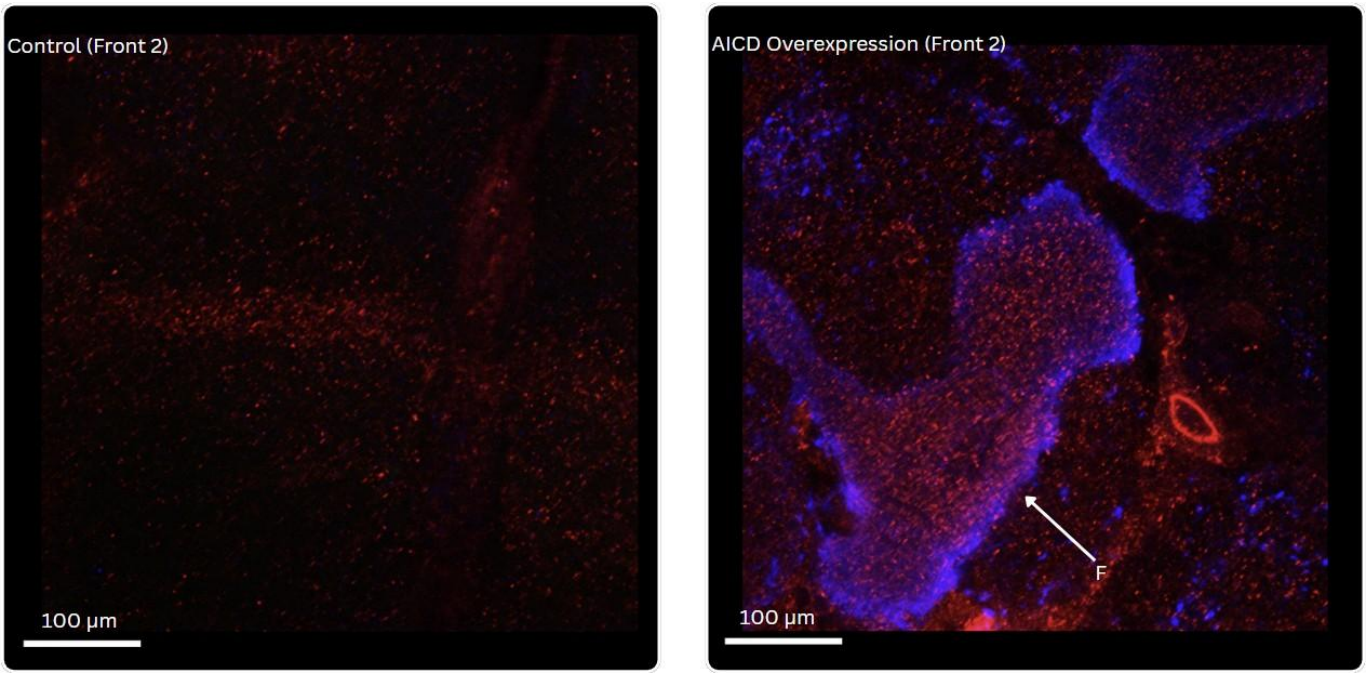

Fig. 1D: Anterior brain region. AICD overexpression yields sharply bounded Arc-positive structures with layered APP at their edges, suggesting Arc-dependent APP trafficking.

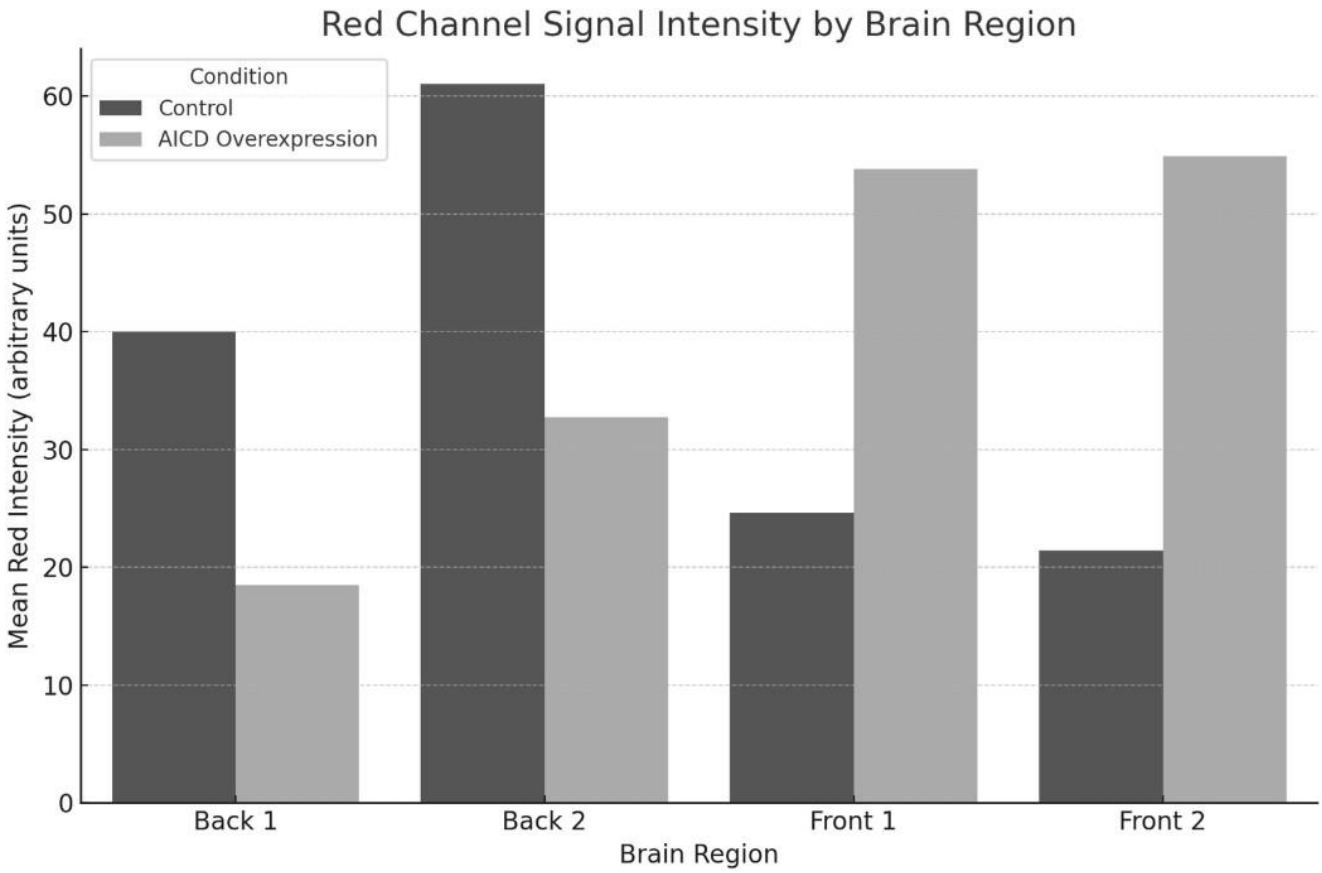

Fig. 1E: Quantified APP fluorescence intensity across brain regions. AICD overexpression reduces global APP levels but drives focal APP aggregation around Arc-expressing neurons.

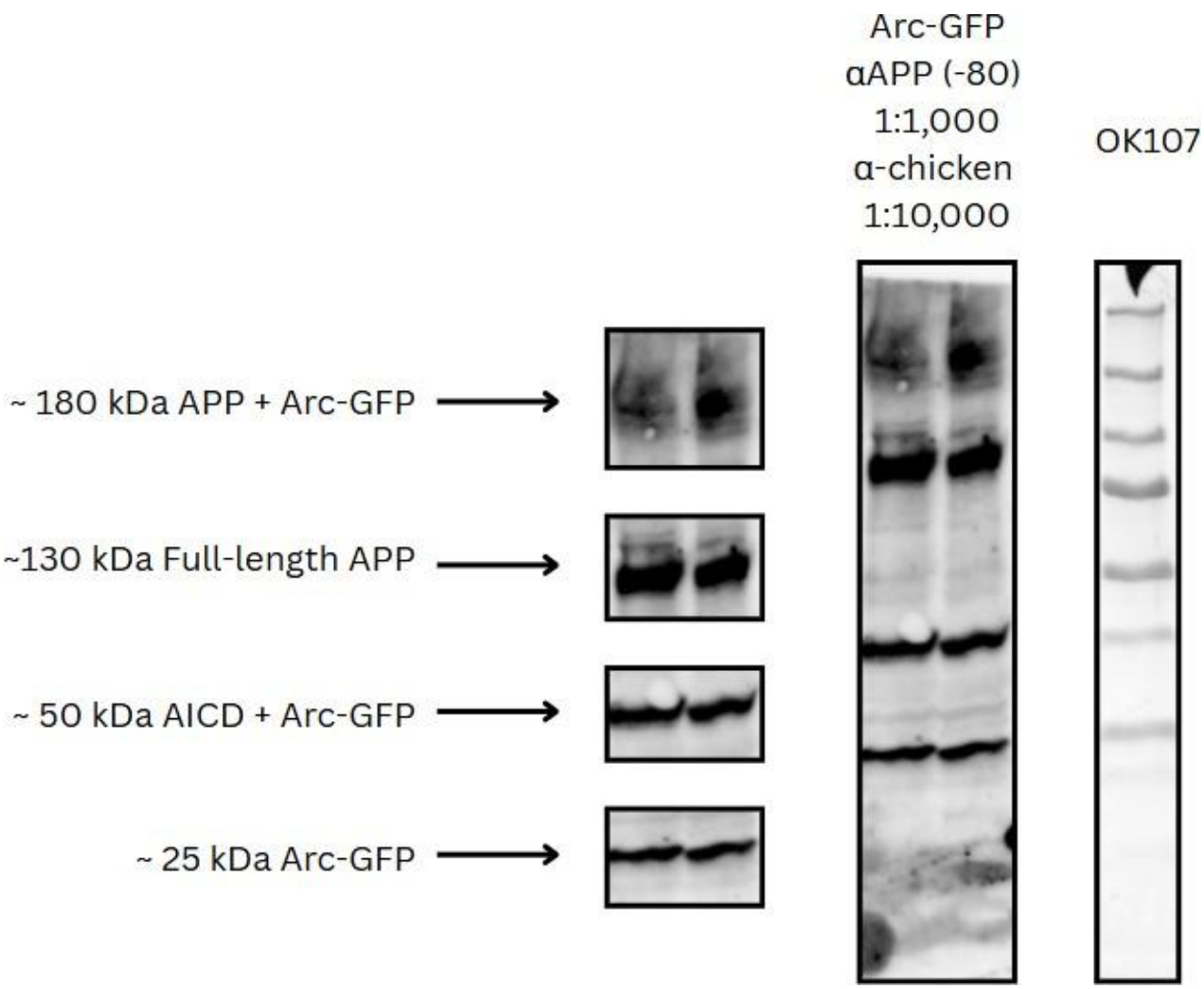

Fig. 2A: Western blot of Drosophila brain lysates showing APP and Arc-GFP species. Molecular-weight markers (kDa) are indicated on the right. Arc-GFP expression alters APP processing and produces additional bands, including a ~180 kDa APP–Arc complex.

of APP. A possible explanation is that the ~180 kDa signal is an APP dimer or higher-order APP oligomer, which is consistent with previous research that APP molecules self-associate under conditions of increased activity in the neurons. Other possible explanations include an APP-Arc complex, where Arc-GFP interacts with the cytoplasmic domains of APP that stabilizes the complex during proteolysis. Future experiments may include co-immunoprecipitation or mass spectrometry to clarify the composition of this higher weight molecular band and determine if it contributes to the feed-forward cleavage loop.

A lower band was also present, and observed to be consistent with AICD. These changes were not present in control brains, which indicates that Arc-GFP facilitates its proteolytic cleavage of stabilization of its fragments.

Further supporting this, Western blotting of MBON-5β neurons with long-term memory (LTM) training revealed that compared to untrained controls, brains from flies trained with LTM exhibited increased levels of APP cleavage products. This includes higher levels of AICD and sAPP, but interestingly as well as the appearance of ~180 kDa APP clusters seen in Western blot 1. These changes were not observed in 5β brains from flies without LTM training, however, which suggests that memory retrieval functions and cognitive processes may increase APP cleavage. The findings suggest a model in which Arc and AICD play huge roles in the pathology of Alzheimer's disease, specifically in continuing the feed-forward loop that induces APP cleavage and further amyloid-beta production.

These results highlight potential future targets for therapeutic intervention by targeting the Arc-AICD interaction. By disrupting the feed-forward loop, excessive APP cleavage and Aβ production could be attenuated, alleviating downstream neurodegenerative processes. The Drosophila model established in this study also provides an adequate in vivo platform for dissecting APP regulation with genetic precision. Results from this system could potentially guide future mammalian research, allowing a robust evaluation of the ability to restore synaptic balance and mitigate Alzheimer's-related pathology by modulating Arc or AICD activity.

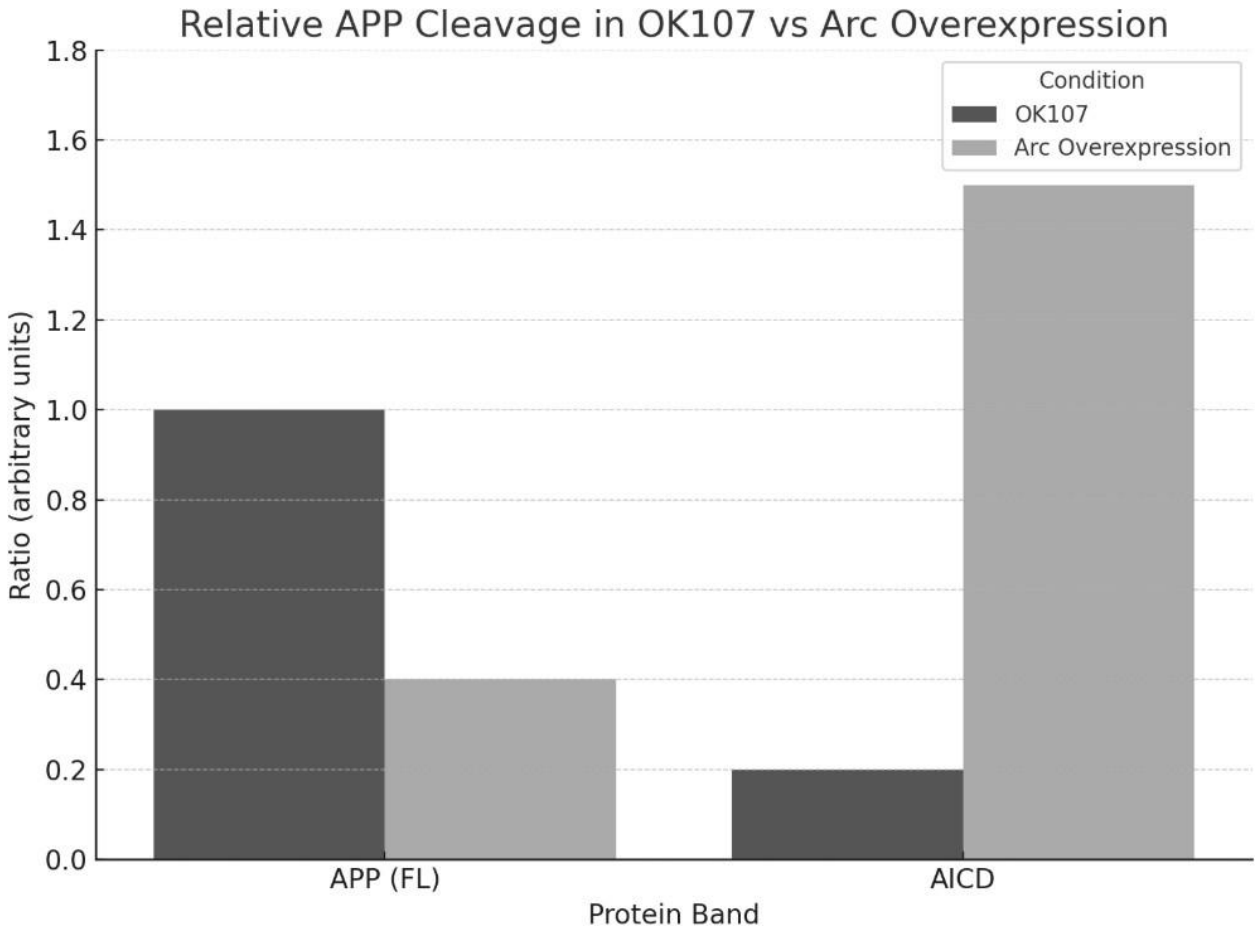

Fig. 2B: Quantification of normalized APP and Arc-GFP band intensities. Arc-GFP overexpression increases APP cleavage prod- ucts relative to control, confirming enhanced proteolytic activity.

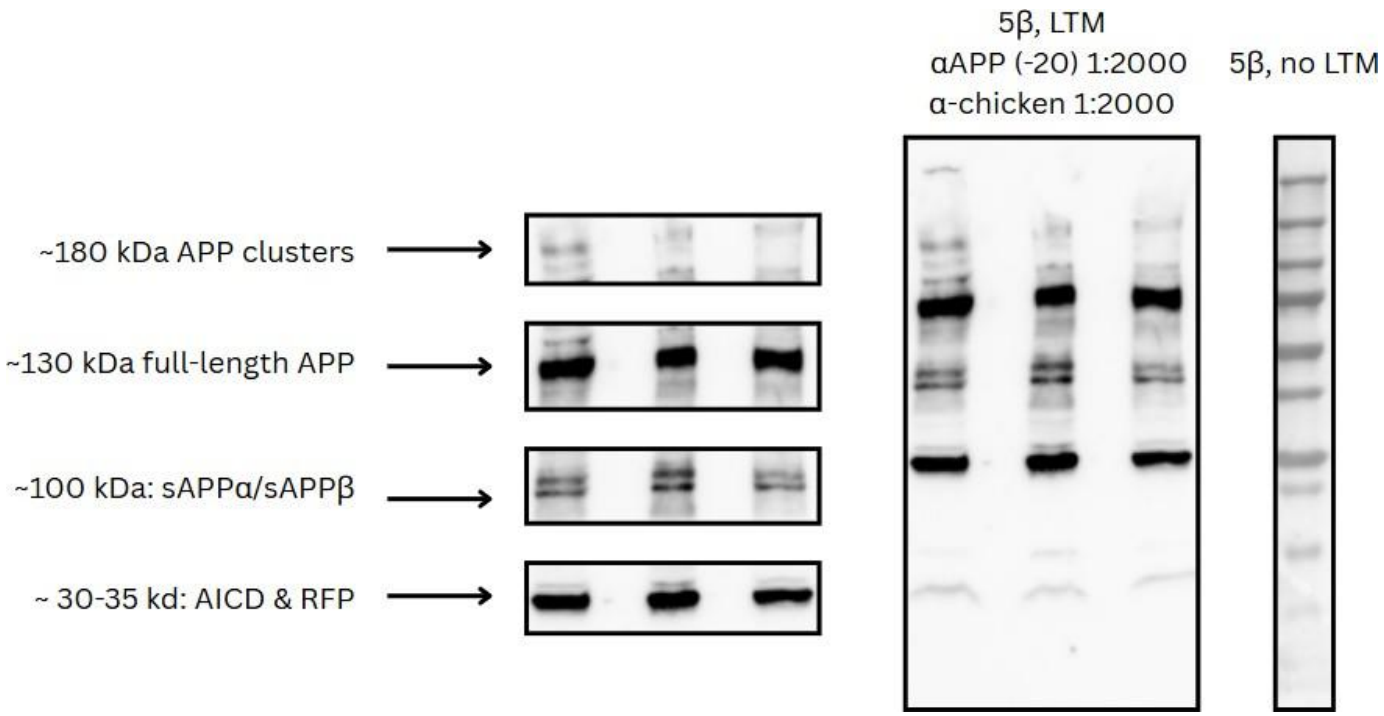

Fig. 3A: Molecular-weight markers (kDa) are indicated on the right. Distinct bands appear at approximately 180 kDa (APP–Arc complex or oligomer), 130 kDa (full-length APP), 50 kDa (AICD + Arc-GFP), and 25 kDa (Arc-GFP)

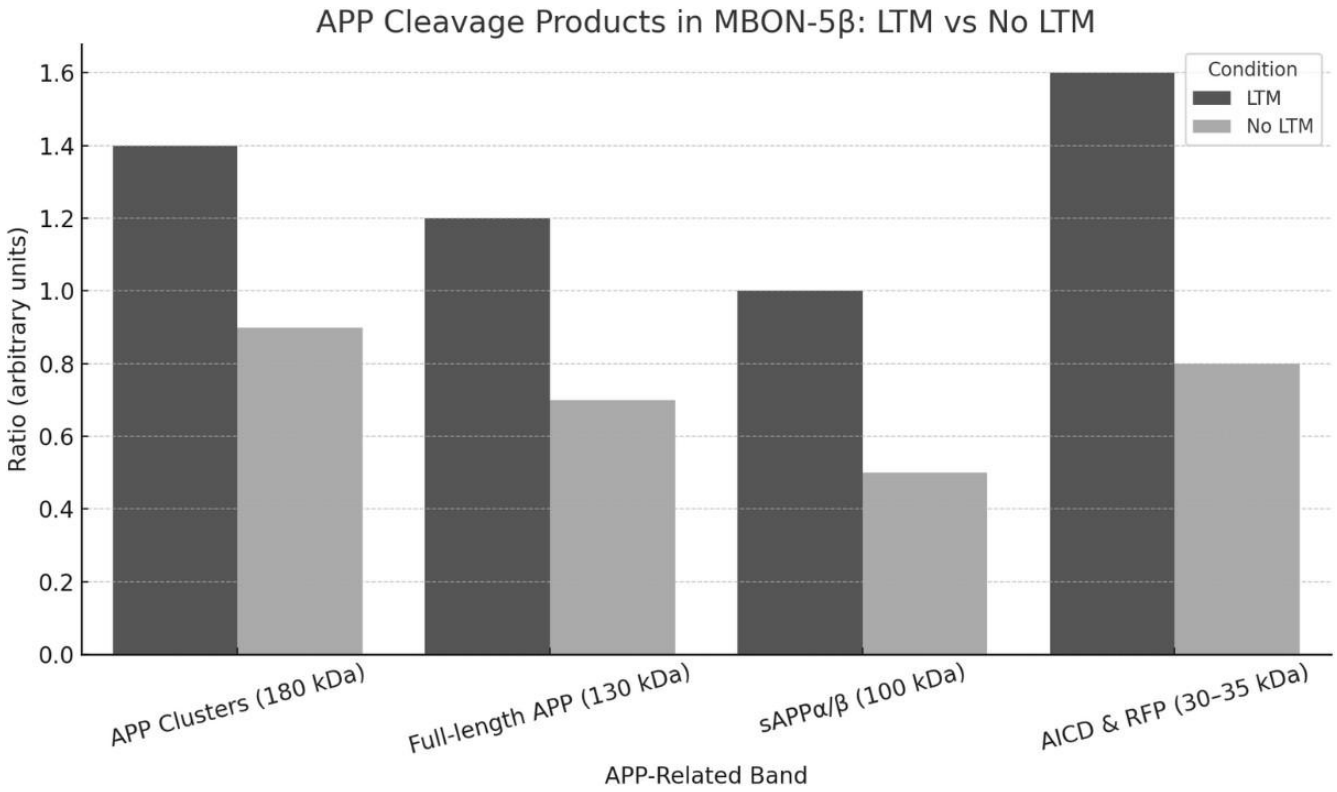

Fig. 3B: Quantification of APP cleavage fragments in MBON-5β neurons. LTM training increases AICD and sAPP intensity, indicating that memory-related neuronal activity enhances APP processing.

9. REFERENCES

Asai, Masashi, et al. “Putative Function of ADAM9, ADAM10, and ADAM17 as APP α-Secretase.” Biochemical and Biophysical Research Communications, vol. 301, no. 1, 2003, pp. 231–235, ISSN 0006-291X. Accessed Jun 24, 2025.

Ashley, James, et al. “Retrovirus-like Gag Protein Arc1 Binds RNA and Traffics across Synaptic Boutons.” Cell, vol. 172, no. 1-2, 2018, pp. 262–274.e11. doi:10.1016/j.cell.2017.12.022. Accessed July 2, 2025.

Chang, Keun-A., et al. “Phosphorylation of Amyloid Precursor Protein (APP) at Thr668 Regulates the Nuclear Translocation of the APP Intracellular Domain and Induces Neurodegeneration.” Molecular and Cellular Biology, vol. 26, no. 11, 2006, pp. 4327–38. doi:10.1128/MCB.02393-05. Accessed May 13, 2025.

Chen, Gf., Xu, Th., Yan, Y., et al. “Amyloid Beta: Structure, Biology and Structure-Based Therapeutic Development.” Acta Pharmacologica Sinica, vol. 38, 2017, pp. 1205–1235, https://doi.org/10.1038/aps.2017.28. Accessed May 13, 2025.

Doig, Andrew J. “Positive Feedback Loops in Alzheimer's Disease: The Alzheimer's Feedback Hypothesis.” Journal of Alzheimer's Disease, vol. 66, no. 1, 2018, pp. 25–36. doi:10.3233/JAD-180583. Accessed May 24, 2025.

Golde, Todd E., et al. “Targeting Abeta and Tau in Alzheimer's Disease, an Early Interim Report.” Experimental Neurology, vol. 223, no. 2, 2010, pp. 252–66. doi:10.1016/j.expneurol.2009.07.035. Accessed Jun 14, 2025.

Hur, J.Y. “γ-Secretase in Alzheimer’s Disease.” Experimental & Molecular Medicine, vol. 54, 2022, pp. 433–446, https://doi.org/10.1038/s12276-022-00754-8. Accessed Jun 18, 2025

Müller, Thorsten, et al. “The Amyloid Precursor Protein Intracellular Domain (AICD) as Modulator of Gene Expression, Apoptosis, and Cytoskeletal Dynamics—Relevance for Alzheimer's Disease.” Progress in Neurobiology, vol. 85, no. 4, 2008, pp. 393–406. doi:10.1016/j.pneurobio.2008.05.002. Accessed Jun 17, 2025.

National Institute on Aging. What Happens to the Brain in Alzheimer’s Disease? U.S. Department of Health and Human Services, 22 May 2024, www.nia.nih.gov/health. Accessed July 1, 2025.

Nhan, Hoang S., et al. “The Multifaceted Nature of Amyloid Precursor Protein and Its Proteolytic Fragments: Friends and Foes.” Acta Neuropathologica, vol. 129, no. 1, 2015, pp. 1–19. doi:10.1007/s00401-014-1347-2. Accessed Jun 17, 2025.

Orobets, K.S., and A.L. Karamyshev. “Amyloid Precursor Protein and Alzheimer’s Disease.” International Journal of Molecular Sciences, vol. 24, no. 19, 2023, p. 14794, https://doi.org/10.3390/ijms241914794. Accessed Jun 12, 2025.

Schulz, Lulu, et al. “Tau-Induced Elevation of the Activity-Regulated Cytoskeleton Associated Protein Arc1 Causally Mediates Neurodegeneration in the Adult Drosophila Brain.” Neuroscience, vol. 518, 2023, pp. 101–111. doi:10.1016/j.neuroscience.2022.04.017. Accessed May 25, 2025.

Zheng, H., and E.H. Koo. “Biology and Pathophysiology of the Amyloid Precursor Protein.” Molecular Neurodegeneration, vol. 6, 2011, p. 27, https://doi.org/10.1186/1750-1326-6-27. Accessed May 25, 2025.